J|A|C|S ARTICLES

Published on Web 08/12/2009

Molecular View of Cholesterol Flip-Flop and Chemical Potential in Different Membrane Environments

W. F. Drew Bennett,[†] Justin L. MacCallum,[†,||] Marlon J. Hinner,[‡] Siewert J. Marrink,[§] and D. Peter Tieleman*[,†]

Department of Biological Sciences, University of Calgary, 2500 University Dr. NW, Calgary, AB T2N 1N4, Canada, Institute of Chemical Sciences and Engineering, Laboratory of Protein Engineering, École Polytechnique Fédérale de Lausanne, CH-1015 Lausanne, Switzerland, and Groningen Biomolecular Sciences and Biotechnology Institute & Zernike Institute for Advanced Materials, University of Groningen, Nijenborgh 4, 9747 AG Groningen, The Netherlands

Received April 30, 2009; E-mail: tieleman@ucalgary.ca

Abstract: The relative stability of cholesterol in cellular membranes and the thermodynamics of fluctuations from equilibrium have important consequences for sterol trafficking and lateral domain formation. We used molecular dynamics computer simulations to investigate the partitioning of cholesterol in a systematic set of lipid bilayers. In addition to atomistic simulations, we undertook a large set of coarse grained simulations, which allowed longer time and length scales to be sampled. Our results agree with recent experiments (Steck, T. L.; et al. *Biophys. J.* **2002**, *83*, 2118−2125) that the rate of cholesterol flip-flop can be fast on physiological time scales, while extending our understanding of this process to a range of lipids. We predicted that the rate of flip-flop is strongly dependent on the composition of the bilayer. In polyunsaturated bilayers, cholesterol undergoes flip-flop on a submicrosecond time scale, while flip-flop occurs in the second range in saturated bilayers with high cholesterol content. We also calculated the free energy of cholesterol desorption, which can be equated to the excess chemical potential of cholesterol in the bilayer compared to water. The free energy of cholesterol desorption from a DPPC bilayer is 80 kJ/mol, compared to 67 kJ/mol for a DAPC bilayer. In general, cholesterol prefers more ordered and rigid bilayers and has the lowest affinity for bilayers with two polyunsaturated chains. Overall, the simulations provide a detailed molecular level thermodynamic description of cholesterol interactions with lipid bilayers, of fundamental importance to eukaryotic life.

Introduction

Cholesterol is an integral and abundant component of mammalian cellular membranes. Cholesterol alters the phase transition of lipid bilayers by smoothing the gel to liquid-crystalline phase transition.[2] At relatively high concentrations of cholesterol, an intermediate liquid-ordered phase, between the liquid-disordered and gel phases, is observed.[2] When compared to the liquid-disordered phase, the liquid-ordered phase is characterized by increased rigidity, hydrophobic thickness, and order.[2] The effect of cholesterol on the phase behavior of membranes is important for putative lipid rafts, lateral domains in cellular membranes enriched in cholesterol and sphingolipids.[3−5] Regions with high cholesterol content would be in the liquid-ordered phase, while the cholesterol-depleted regions would be in the liquid-disordered phase. Lipid rafts are thought to be important for signaling, lipid trafficking, integral membrane protein structure, and behavior.[4] The current consensus of the field defines rafts as small (10−200 nm diameter), highly dynamic, and heterogeneous.[6] Recent evidence has shown giant plasma membrane vesicles[7] and model vesicles (DOPC/DPPC/cholesterol)[8] display critical fluctuations with correlation lengths of ∼20 and 50 nm, which might explain some of the inhomogeneity observed in membranes. The complex driving forces responsible for the ability of cholesterol to modulate lipid phase behavior and raft formation remain poorly understood. We lack an underlying molecular description of cholesterol's behavior in membranes. Currently, there are three major conceptual models for the detailed cholesterol−lipid interactions: the condensed complex model,[9] the superlattice model,[10,11] and the umbrella model.[12] Recently, evidence for both the umbrella model[13] and condensed complex model[14] was provided by determining

[†] University of Calgary.
[‡] École Polytechnique Fédérale de Lausanne.
[§] University of Groningen.
[||] Present address: Department of Pharmaceutical Chemistry, University of California, San Francisco.

(1) Steck, T. L.; Ye, J.; Lange, Y. *Biophys. J.* **2002**, *83*, 2118–2125.
(2) McMullen, T. P. W.; Lewis, R. N. A. H.; McElhaney, R. N. *Curr. Opin. Colloid Interface Sci.* **2004**, *8*, 459–468.
(3) Brown, D. A.; London, E. *Biochem. Biophys. Res. Commun.* **1997**, *240*, 1–7.
(4) Edidin, M. *Annu. Rev. Biophys. Biomol. Struct.* **2003**, *32*, 257–283.
(5) Simons, K.; Ikonen, E. *Nature* **1997**, *387*, 569–572.
(6) Pike, L. J. *J. Lipid Res.* **2006**, *47*, 1597–1598.
(7) Veatch, S. L.; Cicuta, P.; Sengupta, P.; Honerkamp-Smith, A.; Holowka, D.; Baird, B. *ACS Chem. Biol.* **2008**, *3*, 287–293.
(8) Veatch, S. L.; Soubias, O.; Keller, S. L.; Gawrisch, K. *Proc. Natl. Acad. Sci. U.S.A.* **2007**, *104*, 17650–17655.
(9) Radhakrishnan, A.; McConnell, H. M. *Biophys. J.* **1999**, *76*, A431–A431.
(10) Tang, D.; Chong, P. L. G. *Biophys. J.* **1992**, *63*, 903–910.
(11) Somerharju, P. J.; Virtanen, J. A.; Eklund, K. K.; Vainio, P.; Kinnunen, P. K. J. *Biochemistry* **1985**, *24*, 2773–2781.

10.1021/ja903529f CCC: $40.75

the chemical activity of cholesterol in different bilayers, which is related to its chemical potential. Chemical potentials are crucial for predicting lipid phase behavior, as equilibrium requires each species to have a constant chemical potential in all the phases of a system.[15]

In addition, the dynamical aspects of cholesterol in lipid membranes are poorly understood. Global and cellular trafficking of cholesterol and other lipids is a fundamental biological process. In mammals, cholesterol is unevenly distributed between cell types, organelles, and possibly between membrane leaflets.[16] There is a cholesterol concentration gradient along the exocytotic pathway, from the endoplasmic reticulum (0−5 mol %) to the plasma membrane (25−40 mol %).[17] Efficient cholesterol trafficking necessitates that, in addition to diffusing laterally through membranes, cholesterol must undergo intramembrane exchange (flip-flop). A recent study estimated the half-time for cholesterol flip-flop to be <1 s,[1] although earlier estimates were on the minute[18] and even hour[19] range. The rate of cholesterol flip-flop is particularly hard to measure because of the fluid nature of lipid bilayers and the simplicity of cholesterol's structure.

Many computational studies focused on cholesterol and provided valuable insights into the molecular structure and behavior of cholesterol containing bilayers.[20] The concentration-dependent condensing effect of cholesterol has been investigated in molecular dynamics (MD) simulations.[21−23] Of particular interest, Niemela et al. showed that putative rafts have different elastic properties and pressure profiles compared to nonraft bilayers, which provides a possible mechanism of raft function.[24] Using umbrella sampling, Zhang et al. determined potentials of mean force (PMFs) for transferring cholesterol from POPC and sphingomyelin bilayers to water at two temperatures.[25] The thermodynamics of cholesterol transfer from a POPC bilayer to a sphingomyelin bilayer was shown to be energetically favorable but entropically unfavorable.[25] Here, we used all atom (AA) and coarse grained (CG) MD simulations to investigate the thermodynamics of cholesterol partitioning in lipid bilayers. We note that our AA model is a united atom model, lacking aliphatic hydrogens, but does still have atomistic length scale resolution. Free energy landscapes, or PMFs, for cholesterol partitioning from water to the center of the lipid bilayers were calculated using umbrella sampling. We investigated the effect of unsaturated lipid tails with a systematic set of bilayers: dipalmitoyl-PC (DPPC, 16:0−16:0 PC), 1-palmitoyl-2-oleoyl-PC (POPC, 16:0−18:1 PC), 1-stearoyl-2 arachidonyl-PC (SAPC, 18:0−20:4 PC), and diarachidonyl-PC (DAPC, 20:4−20:4 PC). We also simulated DPPC bilayers containing different amounts of cholesterol, using 0, 20, and 40 mol % cholesterol bilayers. The extended time scale accessible by CG simulations allows the direct observation of flip-flop events, while the AA simulations provide atomistic detail. From the PMF, we estimated rates of cholesterol flip-flop and compared them to the directly observed rates from the CG simulations. The relative affinity of cholesterol for the respective bilayers can be inferred from the free energy for desorption, which is equal to the excess chemical potential of cholesterol. For simplicity, we will refer to the bilayers as the phospholipid and the approximate mole percent concentration of cholesterol (C); for example, the DPPC-40%C bilayer.

Methods

AA Simulations. We simulated a DPPC-0%C bilayer (64 DPPCs and two cholesterols), a DPPC-20%C bilayer (52 DPPCs and 12 cholesterols), and a DPPC-40%C bilayer (38 DPPCs and 26 cholesterols). We also investigated a polyunsaturated bilayer using a DAPC-0%C bilayer (72 DAPCs and two cholesterols). The bilayers contained equal concentrations of cholesterol in either leaflet. All the bilayer systems contained 2500−3500 water molecules. We replaced random DPPC molecules from an existing bilayer[26] with cholesterol to obtain the desired concentration and then equilibrated them for at least 50 ns. We calculated the system energy and the area per lipid to monitor equilibration. We added double bonds to an existing bilayer composed of diarachidic-PC (DAPC, 20:0−20:0 PC) to produce diarachidonyl-PC (DAPC, 20:4−20:4 PC). We then equilibrated the bilayer for 50 ns at 323 K. We monitored the equilibration by determining the system energy and the area per lipid.

Simulations were performed with the GROMACS 3.3.1 software package.[27] For DPPC and DAPC, the Berger et al. force field parameters were used.[28] Parameters for the double bonds were from a previous simulation on PLPC[29] and agree with the disorder observed by Feller et al. for a SDPC bilayer.[30] Water was modeled using SPC.[31] Cholesterol was based on the GROMOS87 force field, with minor changes.[32] Bonds were constrained with the LINCS algorithm[33] for DPPC and cholesterol and the SETTLE algorithm[34] for water, allowing a 2-fs time step to be used. Lennard-Jones interactions and electrostatic interactions were cut off at 0.9 nm. The particle mesh Ewald algorithm was used to evaluate long electrostatic interactions.[35,36] The temperatures of water, lipid, and cholesterol were separately kept constant at 323 K using the weak coupling algorithm and a 0.1-ps coupling constant.[37]

(12) Huang, J. Y.; Feigenson, G. W. *Biophys. J.* **1999**, *76*, 2142–2157.
(13) Ali, M. R.; Cheng, K. H.; Huang, J. Y. *Proc. Natl. Acad. Sci. U.S.A.* **2007**, *104*, 5372–5377.
(14) Radhakrishnan, A.; McConnell, H. *Proc. Natl. Acad. Sci. U.S.A.* **2005**, *102*, 12662–12666.
(15) Lee, A. G. *Biochim. Biophys. Acta* **1977**, *472*, 285–344.
(16) Ikonen, E. *Nat. Rev. Mol. Cell Biol.* **2008**, *9*, 125–138.
(17) Sprong, H.; van der Sluijs, P.; van Meer, G. *Nat. Rev. Mol. Cell Biol.* **2001**, *2*, 504–513.
(18) Leventis, R.; Silvius, J. R. *Biophys. J.* **2001**, *81*, 2257–2267.
(19) Backer, J. M.; Dawidowicz, E. A. *Biochim. Biophys. Acta* **1979**, *551*, 260–270.
(20) Berkowitz, M. L. *Biochim. Biophys. Acta* **2009**, *1788*, 86–96.
(21) Hofsass, C.; Lindahl, E.; Edholm, O. *Biophys. J.* **2003**, *84*, 2192–2206.
(22) Chiu, S. W.; Jakobsson, E.; Mashl, R. J.; Scott, H. L. *Biophys. J.* **2002**, *83*, 1842–1853.
(23) Falck, E.; Patra, M.; Karttunen, M.; Hyvonen, M. T.; Vattulainen, I. *Biophys. J.* **2004**, *87*, 1076–1091.
(24) Niemela, P. S.; Ollila, S.; Hyvonen, M. T.; Karttunen, M.; Vattulainen, I. *PLoS Comput. Biol.* **2007**, *3*, 304–312.
(25) Zhang, Z.; Lu, L.; Berkowitz, M. L. *J. Phys. Chem. B* **2008**, *112*, 3807–3811.
(26) Tieleman, D. P.; Marrink, S. J. *J. Am. Chem. Soc.* **2006**, *128*, 12462–12467.
(27) van der Spoel, D.; Lindahl, E.; Hess, B.; Groenhof, G.; Mark, A. E.; Berendsen, H. J. C. *J. Comput. Chem.* **2005**, *26*, 1701–1718.
(28) Berger, O.; Edholm, O.; Jahnig, F. *Biophys. J.* **1997**, *72*, 2002–2013.
(29) Bachar, M.; Brunelle, P.; Tieleman, D. P.; Rauk, A. *J. Phys. Chem. B* **2004**, *108*, 7170–7179.
(30) Feller, S. E.; Gawrisch, K.; MacKerell, A. D., Jr. *J. Am. Chem. Soc.* **2002**, *124*, 318–326.
(31) Berendsen, H. J. C.; Postma, J. P. M.; van Gunsteren, W. F.; Hermans, J. In *Intermolecular Forces*; Pullman, B., Ed.; D. Reidel: Dordrecht, The Netherlands, 1981; pp 331−342.
(32) Holtje, M.; Forster, T.; Brandt, B.; Engels, T.; von Rybinski, W.; Holtje, H. D. *Biochim. Biophys. Acta* **2001**, *1511*, 156–167.
(33) Hess, B.; Bekker, H.; Berendsen, H. J. C.; Fraaije, J. G. E. M. *J. Comput. Chem.* **1997**, *18*, 1463–1472.
(34) Miyamoto, S.; Kollman, P. A. *J. Comput. Chem.* **1992**, *13*, 952–962.
(35) Essmann, U.; Perera, L.; Berkowitz, M. L.; Darden, T.; Lee, H.; Pedersen, L. G. *J. Chem. Phys.* **1995**, *103*, 8577–8593.
(36) Darden, T.; York, D.; Pedersen, L. *J. Chem. Phys.* **1993**, *98*, 10089–10092.
(37) Berendsen, H. J. C.; Postma, J. P. M.; Vangunsteren, W. F.; Dinola, A.; Haak, J. R. *J. Chem. Phys.* **1984**, *81*, 3684–3690.

Semi-isotropic pressure coupling was used with a 2.5-ps coupling constant. The pressure was maintained at 1 bar normal (z-axis) and lateral (xy-plane) to the bilayer plane.[37]

We used umbrella sampling to calculate the PMF for a cholesterol molecule in the AA bilayers (see below). For the 0% DPPC bilayer, we calculated PMFs for cholesterol at 333 and 343 K in addition to the 323 K PMF, to decompose the free energy into entropy/enthalpy components.

CG Simulations. We conducted CG MD simulations with the MARTINI force field,[38] version 2.0, using the standard simulation parameters. All simulations were performed with the GROMACS 3.3.1 software package.[27] We conducted 3-μs equilibrium simulations of DPPC, POPC, SAPC, and DAPC-0%C bilayers (152 PC lipids and two cholesterols). While this is actually 1.3 mol % cholesterol, we will refer to these bilayers as 0%C for brevity. To investigate the effect of cholesterol content, we also simulated a DPPC-40%C bilayer (152 DPPCs and 104 cholesterols). To calculate flip-flop rates, we counted the number of times a cholesterol hydroxyl group crossed from one leaflet to the other. We used umbrella sampling to calculate cholesterol PMFs in CG DPPC, POPC, SAPC, and DAPC-0%C bilayers (64 PC lipids and two cholesterols), as well as a DPPC-40%C bilayer (38 DPPCs and 26 cholesterols).

The Lennard-Jones potentials were shifted from 0.9 to 1.2 nm and cut off after 1.2 nm. Electrostatics were modeled with a Coulombic energy function with explicit screening by using a relative dielectric constant of $\varepsilon = 15$. To mimic the effect of distance-dependent screening, the electrostatic potential was shifted from 0 to 1.2 nm. A temperature of 323 K was used for all systems, with the solvent, lipid, and cholesterol separately coupled with a relaxation time of 0.1 ps.[37] Semi-isotropic, weak pressure coupling[37] was used with a relaxation time of 0.5 ps, and lateral (xy-plane) and normal (z-axis) pressures of 1 bar. We used a 30-fs time step and updated the neighbor list every 10 steps. The simulation time was multiplied by a factor of 4 to give an effective time scale to account for the smoothness of the CG potentials.[38]

Umbrella Sampling. For each bilayer, we simulated 41 windows, with two restrained cholesterols per window, always spaced 4.0 nm apart. By restraining two molecules per window, we doubled the computational efficiency. We showed previously that having two charged arginines separated by 3.7 nm did not significantly affect the PMF in a system of similar size.[39] In the first window, one cholesterol molecule is in bulk water and the other at the bilayer center. In each subsequent window, we moved both cholesterol molecules 0.1 nm in the same direction along the bilayer normal (z-axis), ensuring they were always 4 nm apart. The final window had the first cholesterol at the bilayer center and the other in bulk water on the opposite side of the bilayer. We restrained the hydroxyl of cholesterol with respect to the center of mass of the bilayer, using a harmonic restraint with a force constant of 3000 kJ mol^{-1} nm^{-2} normal to the bilayer. PMFs were calculated using the weighted histogram analysis method.[40] We calculated the mean PMF and its standard error using the two PMFs for the independent cholesterol molecules, one through either leaflet. The AA simulations were run for 20−40 ns, depending on convergence of the PMFs. For the CG umbrella sampling, each window was run for 150 ns.

We calculated PMFs for CHOL partitioning through AA DPPC bilayers at three temperatures (323, 333, and 343 K) to decompose the free energy into entropy and enthalpy contributions. Using the centered difference method outlined in[41]

$$-T\Delta S \approx \frac{T}{2\Delta T}[G(T + \Delta T) - G(T - \Delta T)] \quad (1)$$

we can estimate the entropy contribution ($-T\Delta S$) to the PMF.

Using the formula

$$\Delta H = \Delta G + T\Delta S \quad (2)$$

we can use the entropy calculated above to estimate the enthalpy contribution (ΔH).

Results

PMFs. Partial density profiles for the AA DPPC-0%C, DPPC-20%C, and DPPC-40%C bilayers are shown in Figure 1A. As expected, the bilayer becomes thicker (Figure 1A) and the area per lipid decreases (Table 1) as the concentration of cholesterol increases. Additionally, the area per lipid increases as we increase the number of double bonds in the acyl tails (Table 1).

We calculated PMFs for transferring cholesterol from water to the center of AA (Figure 1B) and CG bilayers (Figure 1C). There are free energy troughs at the equilibrium position of cholesterol in the bilayers. As the order and rigidity of the bilayer are increased, the position of the trough moves farther from the bilayer center, consistent with an increase in the thickness of the bilayer. All of the bilayers have similar smooth slopes, as cholesterol desorbs from the bilayer into bulk water. The PMFs flatten when the tail of cholesterol stops interacting with the bilayer. There is also a steep slope in the PMFs from equilibrium toward the center of the bilayer. After reaching the free energy barrier, as we move cholesterol farther into the bilayer, the PMF plateaus or decreases slightly, as for the CG DPPC-40%C bilayer. Table 1 summarizes the major free energy features of the PMFs.

Flip-Flop Rates. We calculated rates for cholesterol flip-flop using

$$k_f = k_d \times \exp(-\Delta G_{center}/RT)$$

where ΔG_{center} is the difference in free energy between the bilayer center (z_{center}) and the cholesterol equilibrium position (z_{eq}), k_d is the rate cholesterol moves from z_{center} to z_{eq}, and k_f is the rate cholesterol moves from z_{eq} to z_{center}. To estimate k_d, we released the harmonic restraint on a cholesterol at z_{center} and determined the time it takes to return to z_{eq}. This process has a large stochastic element because the PMFs have a broad plateau near the bilayer center, which cholesterol must diffuse across to reach z_{eq}. In some of the bilayers, such as the CG DPPC-40%C bilayer, there is even a free energy barrier cholesterol must overcome to reach its equilibrium position. Instead of attempting a more rigorous estimate, we estimated a range of rates using the upper and lower values of k_d from 10 separate simulations. Using both the observed k_d and the calculated k_f rates, we can now determine the rate of flip-flop (k_{flip})

$$k_{flip} = \frac{1}{k_f^{-1} + k_d^{-1}} \times \frac{1}{2}$$

A complete flip-flop involves the rate to move from equilibrium to the bilayer center (k_f) and the rate to move from the center to the opposite leaflet (k_d). The factor of one-half accounts for cholesterol molecules that reach the bilayer center only to return to their original leaflet.

Both the AA and CG models predict that as the order and rigidity of the bilayer increase, the rate of cholesterol flip-flop decreases by orders of magnitude (Table 1). Using the CG model allowed

(38) Marrink, S. J.; Risselada, H. J.; Yefimov, S.; Tieleman, D. P.; de Vries, A. H. *J. Phys. Chem. B* **2007**, *111*, 7812–7824.
(39) MacCallum, J. L.; Bennett, W. F. D.; Tieleman, D. P. *Biophys. J.* **2008**, *94*, 3393–3404.
(40) Kumar, S.; Bouzida, D.; Swendsen, R. H.; Kollman, P. A.; Rosenberg, J. M. *J. Comput. Chem.* **1992**, *13*, 1011–1021.
(41) MacCallum, J. L.; Tieleman, D. P. *J. Am. Chem. Soc.* **2006**, *128*, 125–130.

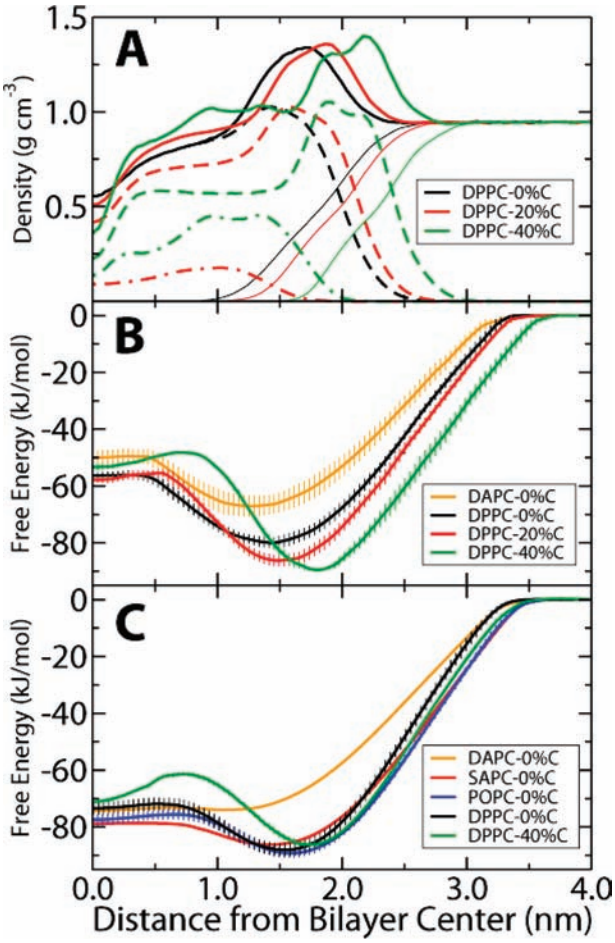

Figure 1. Cholesterol free energy profiles. (A) Partial density profiles of the AA 0%, 20%, and 40% DPPC bilayers. Total density is solid thick lines, water density is solid thin lines, DPPC density is thick dashed lines, and cholesterol density is dot-dashed lines. (B) PMFs for cholesterol partitioning in the AA bilayers. (C) CG PMFs for cholesterol partitioning from water to the center of various bilayers. Both AA and CG PMFs were set equal to zero in bulk water. Error bars are the standard error from the mean of the two leaflets cholesterol PMFs.

cholesterol flip-flop to be directly observed in equilibrium simulations (Figure 2). The directly observed CG rates are within our calculated range of rates for all the CG bilayers, demonstrating that our method of estimation is reasonable (Table 1).

Cholesterol Orientation and Snapshots. Because of the long and rigid structure of cholesterol, it is interesting how it is oriented in the bilayer at equilibrium, as well as during flip-flop and desorption. We defined a vector from the hydroxyl of cholesterol to the carbon joining the rings and tail. For each umbrella window, we calculated histograms for the angle the vector of cholesterol forms with the bilayer normal throughout the simulation. Using the formula

$$\Delta G = -RT \ln(\alpha)$$

we converted the normalized histograms (α) into free energies. Combining each umbrella window's histogram, we created a free energy landscape for the preferential angle distribution of cholesterol as it partitioned into each bilayer (Figure 3). The minimum free energy is the most probable orientation of cholesterol in the bilayer at a particular depth with respect to the bilayer normal. As the order and rigidity of the bilayer increase, the average tilt angle of cholesterol at the equilibrium position becomes smaller (Table 1).

Table 1. Structural, Thermodynamic, and Kinetic Properties of Lipid/Cholesterol Bilayers

			observed			calculated		observed
lipid	A/L (nm^2)	Θ_{equil}[a] (deg)	ΔG_{desorb} (kJ/mol)[b]	$\Delta G_{barrier}$ (kJ/mol)[c]	ΔG_{center} (kJ/mol)[d]	t_d (ns)[e]	k_d (s^{-1})[f]	k_f (s^{-1})[g]	k_{flip} (s^{-1})[h]	k_{flip} (s^{-1})[i]
CG DAPC-0%C	0.89	30	74	1	0	1.6 to 10.8	9.3×10^7 to 6.3×10^8	9.3×10^7 to 6.3×10^8	2.3×10^7 to 1.6×10^8	$7.5 \times 10^7 \pm 0.2 \times 10^7$
CG SAPC-0%C	0.79	27	86	7	7	2 to 10.4	9.6×10^7 to 5.0×10^8	7.1×10^6 to 3.7×10^7	3.3×10^6 to 1.7×10^7	$6.7 \times 10^6 \pm 0.5 \times 10^6$
CG POPC-0%C	0.66	23	89	13	12	1.2 to 18.8	5.3×10^7 to 8.3×10^8	6.1×10^5 to 9.5×10^6	3.0×10^5 to 4.7×10^6	$1.5 \times 10^6 \pm 0.3 \times 10^6$
CG DPPC-0%C	0.62	23	88	16	15	1.2 to 16	6.3×10^7 to 8.3×10^8	2.3×10^5 to 3.1×10^6	1.2×10^5 to 1.6×10^6	$7.4 \times 10^5 \pm 2.1 \times 10^5$
CG DPPC-40%C	0.44	15	86	25	15	6.4 to 258.8	3.9×10^6 to 1.6×10^8	1.4×10^4 to 5.9×10^5	7.2×10^3 to 2.5×10^4	$>1.4 \times 10^4$
AA DAPC-0%C	0.87	33	67	18	17	0.2 to 1.7	5.9×10^8 to 4.2×10^9	1.0×10^6 to 7.4×10^6	5.2×10^5 to 3.7×10^6	
AA DPPC-0%C	0.64	29	80	24	24	0.1 to 5.5	1.8×10^8 to 1.0×10^{10}	2.4×10^4 to 1.3×10^6	1.2×10^4 to 6.6×10^5	
AA DPPC-20%C	0.56	19	86	31	28	0.6 to 40.0	2.5×10^7 to 1.7×10^9	2.4×10^2 to 1.6×10^4	1.2×10^3 to 8.1×10^3	
AA DPPC-40%C	0.43	13	89	41	36	1.5 to >80	1.3×10^7 to 6.7×10^8	1.9×10^1 to 1.0×10^3	9.4 to 5.0×10^2	

[a] Average tilt angle of cholesterol at its equilibrium position. [b] Free energy barrier for desorption, from the PMFs. [c] Free energy barrier for flip-flop, for moving cholesterol from equilibrium to the bilayer center. [d] Free energy difference between equilibrium and the bilayer center. [e] t_d was estimated by releasing the restraint on cholesterol at the bilayer center and measuring the time it took to return to equilibrium. [f] Observed rate for cholesterol to move from the center of the bilayer to equilibrium, $k_d = t_d^{-1}$. [g] Calculated rate for cholesterol to reach the center of the bilayer, from $k_f = k_d \times \exp(-\Delta G/RT)$. [h] Calculated rate for cholesterol flip-flop, $k_{flip} = 1/[(1/k_f) + (1/k_d)] \times 1/2$. [i] Rate of flip-flop observed during equilibrium simulations, $k_{flip} \pm$ SEM (see Supporting Information). The slow rate of flip-flop in the DPPC-40%C bilayer prevented us from obtaining a reliable observed rate from 3-μs equilibrium simulations.

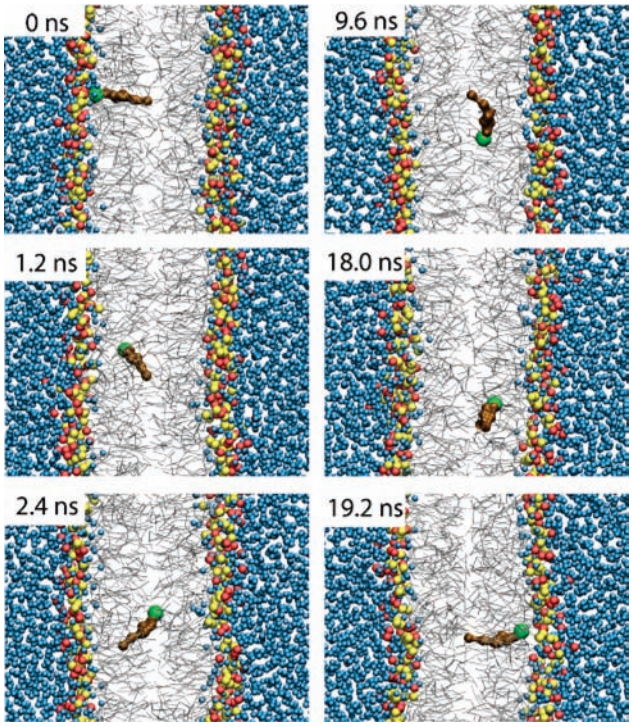

Figure 2. Cholesterol flip-flop. Snapshots illustrating cholesterol flip-flop in a CG DPPC-0%C bilayer during an equilibrium simulation. Water particles are blue spheres, the DPPC cholines are red spheres, their phosphates are yellow spheres, and their tails are gray lines. The body of cholesterol is brown licorice, and its hydroxyl is a green sphere. Time equal to 0 ns corresponds to right before the hydroxyl of cholesterol enters the hydrophobic interior, at 1.2 μs of simulation.

Cholesterol has much greater orientation freedom at the bilayer center compared to equilibrium (Figure 3). At the center of the bilayer, cholesterol rotates freely, with its tail in either leaflet equally, as well as lying perpendicular to the bilayer normal. Figure S3A,B in the Supporting Information shows snapshots of cholesterol at the center of AA and CG DPPC-0%C bilayers, with its long axis perpendicular to the bilayer normal. There is a clear ordering trend observed in the angle PMFs from the DPPC-0%C to the DPPC-40%C bilayer (Figure 3). As cholesterol content is increased, cholesterol molecules are more restricted, although even in the ordered DPPC-40%C bilayer cholesterol can rotate between 0 and 180° at the bilayer center.

In bulk water, there is no orientational preference for cholesterol. For all the bilayers, a clear transition between cholesterol floating in bulk water and interacting with the bilayer is shown by an abrupt change from randomly to strongly oriented as cholesterol approaches the bilayer. Figure S3C,D in the Supporting Information shows snapshots of the AA and CG DPPC-0%C bilayer at the maximum distance that cholesterol still interacts with the bilayer.

Enthalpy/Entropy Decomposition. Figure 4 shows the free energy decomposition for the AA cholesterol PMF in the DPPC-0%C bilayer at 333 K. The transfer of cholesterol from water to its equilibrium position in a DPPC bilayer has a favorable ΔG_{desorb} of 75 kJ/mol, the sum of an unfavorable $-T\Delta S_{\text{desorb}}$ of transfer of 77 kJ/mol, and a favorable ΔH_{desorb} of 152 kJ/mol. The ΔG_{center} for cholesterol in a DPPC bilayer is 23 kJ/mol, of which there is an unfavorable ΔH_{center} of 74 kJ/mol and a favorable $-T\Delta S_{\text{center}}$ of 51 kJ/mol. Near the bilayer center, ΔG, ΔH, and $-T\Delta S$ all plateau. This corresponds to the breaking

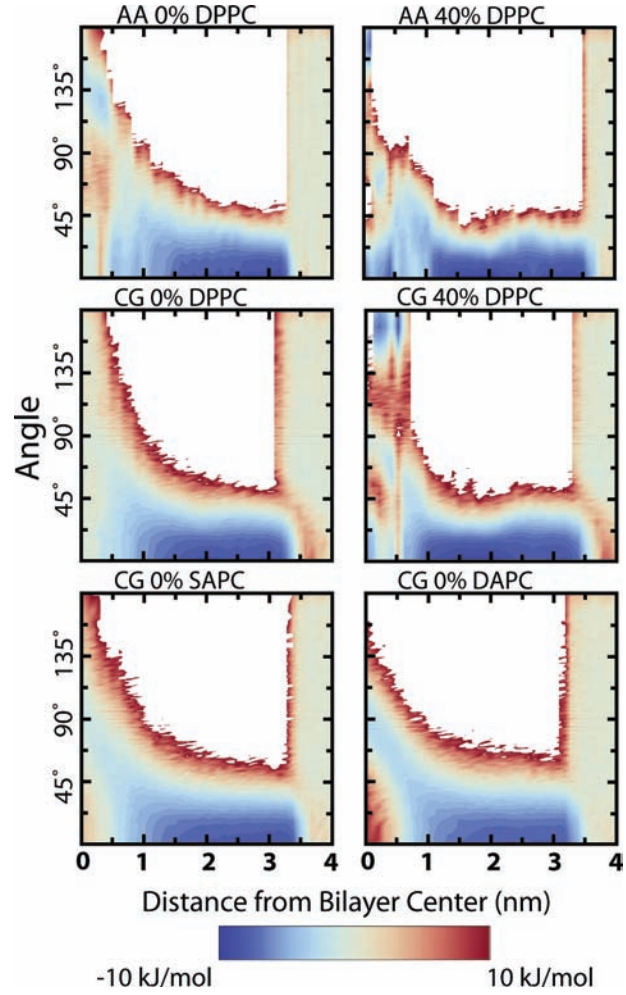

Figure 3. Free energy landscapes for the angle cholesterol forms with the bilayer normal as it partitions through AA and CG bilayers. We calculated histograms of the angle formed by the z-axis and a vector from the hydroxyl of cholesterol to the carbon joining its rings and tail throughout the simulations. Using $\Delta G = -RT\ln(\alpha)$, we converted the normalized histograms into free energies.

of the transient water defect, when the number of hydrogen bonds to cholesterol drops to zero (Figure S1 in the Supporting Information). Overall, the transfer from water to the center of the bilayer has a favorable ΔG of 52 kJ/mol and notably an unfavorable $-T\Delta S$ of 26 kJ/mol.

Discussion

CG vs AA. By using two separate models, at different levels of detail, we describe the thermodynamics of cholesterol equilibrium stability in lipid bilayers as well as its fluctuations from equilibrium. Given the complexity of cholesterol partitioning in lipid bilayers and the semiquantitative nature of the MARTINI model, we feel the agreement between the two models is satisfactory. Using the CG model, we were able to access time scales on which we predict cholesterol flip-flop to occur. The directly observed rates are in good agreement with predicted rates from umbrella sampling. Despite qualitative differences between the flip-flop rates, the overall trend is clear; increasing the order and rigidity decreases the rate of cholesterol flip-flop by orders of magnitude. Additionally, from the angle PMFs and snapshots, the mechanism of cholesterol flip-flop, desorption, and equilibrium stability is consistent between the AA and CG models. Quantitative analysis shows the two models

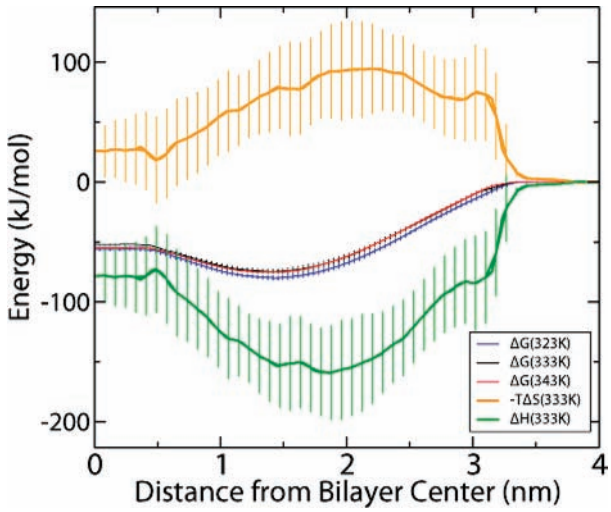

Figure 4. Free energy decomposition for cholesterol in a DPPC bilayer. The PMF for moving cholesterol from water into the center of a 0% DPPC bilayer decomposed into entropy and enthalpy contributions. We decomposed the PMF at 333 K using eq 1.

do differ in some important respects and suggests possible improvements for both force fields (see Supporting Information).

Flip-Flop. We showed that cholesterol flip-flops across lipid bilayers on a very short time scale. Rapid cholesterol flip-flop has important implications on cellular and global cholesterol trafficking. It was shown that cholesterol flip-flop occurs on a time scale of <1 s in a human red cell.[1] Our results agree that the rate of cholesterol flip-flop is fast, generally on a time scale of <1 s. The fast flip-flop of cholesterol implies that passive translocation would be physiologically important. Maintaining an asymmetric distribution of cholesterol between membrane leaflets using cholesterol flippases or floppases would be difficult and energy consuming. Fast flip-flop suggests the transbilayer distribution of cholesterol could approach equilibrium on a physiological time scale and therefore would be governed by its chemical potential in each of the respective leaflets (see Chemical Potential). This is in contrast to phospholipids, which have been shown to have slow rates of spontaneous flip-flop (half times of hours to days)[26,42−44] and therefore are unlikely to reach equilibrium distributions on physiological time scales. From the slow rate of passive phospholipid flip-flop, it is generally assumed that protein-mediated translocation must occur.[45]

By using computer simulations, we can control the local composition of the bilayers and calculate bilayer-dependent cholesterol flip-flop rates. We predict that there is a large gradient in flip-flop rates, with respect to the bilayers' structure and fluidity. For example, in a cholesterol-depleted domain enriched in polyunsaturated lipids, cholesterol would flip around a million times more often than in a rigid, cholesterol-enriched domain. Recent neutron scattering data showed that cholesterol even prefers the center of polyunsaturated (DAPC) bilayers,[46] which is supported by the CG results as presented here and in previous work.[47,48] AA simulation results comparing cholesterol behavior in long-tail and short-tail PC lipids also provided evidence for a composition-dependent flip-flop rate.[49] Clearly, a single estimate for the rate of cholesterol flip-flop is not adequate for understanding cellular cholesterol trafficking.

From the free energy decompositions, the simulation snapshots, and the angle PMFs, we showed an in-depth analysis of the mechanism of cholesterol flip-flop. The ΔG for transferring cholesterol from equilibrium to the bilayer center was due to an unfavorable ΔH_{center} and a favorable $-T\Delta S_{center}$. The plateau of the PMF corresponds to the desolvation of cholesterol (see Supporting Information). Róg et al. showed that by changing the hydroxyl headgroup of cholesterol to a ketone the hydration of the sterol was 4 times lower, and flip-flop events were observed during a 200-ns AA equilibrium simulation.[50] The observed unfavorable ΔH_{center} for flip-flop is likely due to the desolvation of cholesterol's headgroup. A control simulation of a cholesterol analogue molecule, which lacked a hydroxyl headgroup (see Supporting Information), supports this assertion.

Chemical Potential. Equating the free energy of desorption to the excess chemical potential of cholesterol in the bilayer compared to water allows the relative affinity of cholesterol for the different bilayers to be inferred. Recently, Zhang et al. used a similar approach to demonstrate that cholesterol has a higher affinity for sphingomyelin than POPC.[25] Their results showed that the transfer of cholesterol from POPC to sphingomyelin was exothermic, which agreed qualitatively with calorimetric data.[51] Our results show that cholesterol has the lowest affinity for bilayers with two polyunsaturated tails. We find this for both the AA and CG levels of resolution. The low affinity of cholesterol for polyunsaturated lipid tails has been demonstrated experimentally using cyclodextrin cholesterol extraction[18] and fluorescence microscopy[52] and has been suggested by MD simulations.[48,53] Cholesterol's preference for rigid, ordered bilayers could be a driving force for lateral domain formation, as well as general cholesterol cellular movement down the exocytotic pathway. We found the chemical potential of cholesterol in the AA DPPC-0%C bilayer to be −80 kJ/mol, compared to −89 kJ/mol for the AA DPPC-40%C bilayer. Therefore, transferring cholesterol from the AA DPPC-0%C bilayer to the DPPC-40%C bilayer would be favorable by 9 kJ/mol. Although we find cholesterol prefers more ordered, rigid bilayers with high cholesterol content, we do not assume the trend would continue if we further increased the concentration of cholesterol in a DPPC bilayer. Experimental evidence using a cholesterol oxidase activity assay showed a jump in the chemical activity of cholesterol in a DPPC bilayer when the mole fraction of cholesterol exceeded 0.57.[13]

An estimate of 116 kJ/mol for cholesterol desorption from a red cell was determined using β-dextrin as an acceptor.[1] We showed that, although somewhat larger than our estimate in the range of 80−90 kJ/mol, the free energy for desorption is strongly

(42) Wimley, W. C.; Thompson, T. E. *Biochemistry* **1990**, *29*, 1296–1303.
(43) De Kruijff, B.; van Zoelen, E. J. *Biochim. Biophys. Acta* **1978**, *511*, 105–115.
(44) Kornberg, R. D.; McConnell, H. M. *Biochemistry* **1971**, *10*, 1111–1120.
(45) Daleke, D. L. *J. Lipid Res.* **2003**, *44*, 233–242.
(46) Harroun, T. A.; Katsaras, J.; Wassall, S. R. *Biochemistry* **2006**, *45*, 1227–1233.
(47) Marrink, S. J.; de Vries, A. H.; Harroun, T. A.; Katsaras, J.; Wassall, S. R. *J. Am. Chem. Soc.* **2008**, *130*, 10–11.
(48) Risselada, H. J.; Marrink, S. J. *Proc. Natl. Acad. Sci. U.S.A.* **2008**, *105*, 17367–17372.
(49) Kucerka, N.; Perlmutter, J. D.; Pan, J.; Tristram-Nagle, S.; Katsaras, J.; Sachs, J. N. *Biophys. J.* **2008**, *95*, 2792–2805.
(50) Róg, T.; Stimson, L. M.; Pasenkiewicz-Gierula, M.; Vattulainen, I.; Karttunen, M. *J. Phys. Chem. B* **2008**, *112*, 1946–1952.
(51) Tsamaloukas, A.; Szadkowska, H.; Heerklotz, H. *Biophys. J.* **2006**, *90*, 4479–4487.
(52) Mitchell, D. C.; Litman, B. J. *Biophys. J.* **1998**, *75*, 896–908.
(53) Pitman, M. C.; Suits, F.; MacKerell, A. D., Jr.; Feller, S. E. *Biochemistry* **2004**, *43*, 15318–15328.

dependent on the composition and structure of the bilayer. The composition of a human red cell is much more complex than our two component mixtures. In addition, real biological membranes have an asymmetric distribution of lipids between the two leaflets. Our finding that the chemical potential of cholesterol depends on the structure and composition of the bilayer implies that bilayers with an asymmetric distribution of lipids will have an asymmetric distribution of cholesterol. Recently, it was shown that the distribution of the sterols, dehydroergosterol and cholestatrienol, in living cells is asymmetric, with sterol enrichment on the cytoplasmic leaflet.[54] This finding goes against the traditional view of sterol preference for sphingomyelin, which is enriched on the extracellular leaflet. Future calculations similar to the ones presented here might help elucidate this discrepancy, although other in vivo mechanisms, such as lipid metabolism and large-scale membrane rearrangements, likely also play a role in the distribution of cholesterol.

Free Energy Decompositions. The free energy decomposition showed that the favorable ΔG for transferring cholesterol from water to the DPPC bilayer was due to a large favorable ΔH and an unfavorable $-T\Delta S$. We decomposed the PMF at 333 K because the melting temperature of DPPC is 314 K,[55] making decomposition using the centered difference method at 323 K problematic. From the hydrophobic effect, and cholesterol's bulky, hydrophobic body, we would expect its transfer from water to a hydrophobic environment to be entropy driven. To help explain our PMF decomposition, we note that the hydrophobic effect is temperature-dependent. Cholesterol is also slightly amphipathic, with a polar hydroxyl headgroup, which would affect its PMF. As well, because of the length of cholesterol, the center of a DPPC bilayer is an inhomogeneous environment. Therefore, as a control, we determined PMFs for the transfer of cholesterol from water to an octane slab (see Supporting Information). We found that at 333 K the ΔG of transfer from water to octane was -70 kJ/mol and had an unfavorable $-T\Delta S$ of 72 kJ/mol, both qualitatively similar to the DPPC bilayer decomposition. There is a strong temperature dependence of $-T\Delta S$, and we note that, at 313 K, $-T\Delta S$ is favorable. The octane PMFs show that thermodynamically the transfer of cholesterol from water to the center of a DPPC bilayer is similar to an alkane solvent, and that the unfavorable $-T\Delta S$ may be due to the high temperature or particular cholesterol−water interactions. In general, the thermodynamics of cholesterol transfer from water to a hydrophobic environment is complex, but critically important for understanding cholesterol homeostasis.

(54) Mondal, M.; Mesmin, B.; Mukherjee, S.; Maxfield, F. R. *Mol. Biol. Cell* **2009**, *20*, 581–588.
(55) Biltonen, R. L.; Lichtenberg, D. *Chem. Phys. Lipids* **1993**, *64*, 129–142.

Conclusions

We used both CG and AA computer simulations to investigate cholesterol transfer from water to its equilibrium position in the membrane and to the center of the membrane for a systematic set of lipid bilayers. The AA model allowed detailed free energy decomposition and insights into the molecular driving forces. The CG simulations provided a valuable link from our biased simulations to an equilibrium rate. In agreement with experiment, we found that the rate of cholesterol flip-flop is fast on physiological time scales. We predict that the rate varies greatly depending on the bilayer properties; increasing the order and reducing the fluidity caused the rate to decrease by orders of magnitude. Comparing the free energy barriers for desorption of cholesterol shows that cholesterol prefers ordered, rigid bilayers enriched in cholesterol. In particular, cholesterol had the lowest affinity for bilayers with two polyunsaturated tails. These results open the way to a detailed, thermodynamically based description of lipid/cholesterol mixtures, which is much needed to enhance our understanding of biomembrane-related processes.

Acknowledgment. This work was supported by the National Sciences and Engineering Research Council (NSERC). W.F.D.B. was supported by studentships from NSERC and AHFMR. J.L.M. was supported by fellowships from NSERC and AHFMR. M.J.H. received a short-term postdoctoral fellowship from the German Academic Exchange Service DAAD. D.P.T. is an Alberta Heritage Foundation for Medical Research Senior Scholar and Canadian Institutes of Health Research New Investigator.

Supporting Information Available: CG vs AA models, enthalpy and entropy decomposition, snapshots of cholesterol at the center of AA and CG DPPC-0%C bilayers, PMFs for the transfer of cholesterol from water to octane slab. This material is available free of charge via the Internet at http://pubs.acs.org.

JA903529F